

## ***Supplementary Material***

# **Terahertz metasurface biosensor based on electromagnetically induced transparency for fingerprint trace detection**

**Rong Zhao<sup>1†</sup>, Qiang Niu<sup>1†</sup>, Yi Zou<sup>1</sup>, Bin Cui<sup>1,2</sup> and Yuping Yang<sup>1,2\*</sup>**

<sup>1</sup>School of Science, Minzu University of China, Beijing 100081, China

<sup>2</sup>Engineering Research Center of Photonic Design Software, Ministry of Education, Beijing 100081, China

<sup>†</sup>These authors contributed equally to this work.

\*ypyang@muc.edu.cn

**This PDF file includes Supplementary Fig. S1-S3**

### Supplementary Fig. S1

In order to further explore the electromagnetic characteristic for the proposed EIT metasurface biosensors, the surface current and electric field energy density at the Dip 1, peak and Dip 2 are drawn in the Fig. S1 for further exploration. It can be seen that Dip1 and Dip2 are mainly dominated by the element 2 and 1, respectively. In the case of the transparency peak, electric field distribution is highly concentrated at the gaps of element 2, and suppressed at element 1, which is consistent with three level system in quantum EIT involved a ground state and two excited states.

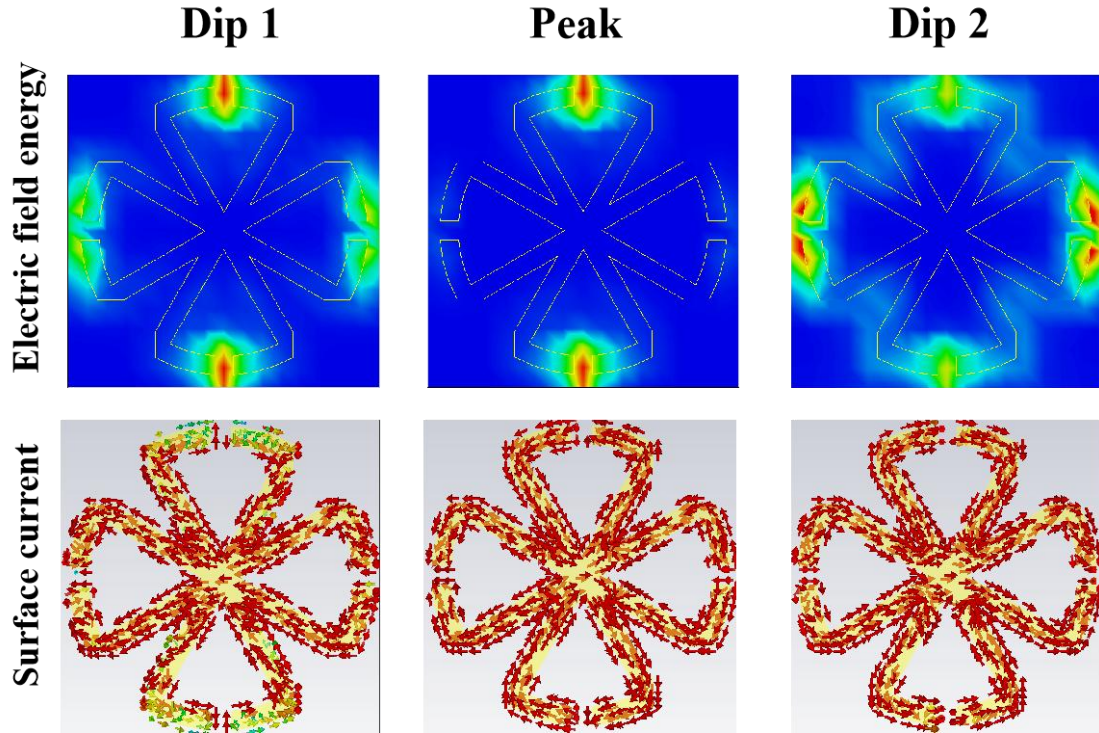


Fig. S1. The surface current and electric field energy density at the Dip 1, Dip 2 and peak.

### Supplementary Fig. S2

The transmission spectra, caused by rotational perturbations within  $45^\circ$  at the steps of  $5^\circ$ , are used to explore its polarization insensitivity. It can be seen in Fig. S2a that no significant change can be observed. In addition, the corresponding relative changes in resonant frequency and amplitude were further recorded, which show the signal changes within 2%, as shown in the Fig. S2b. It is worth noting that the proposed metasurface achieves the all-angle ( $360^\circ$ ) polarization insensitivity stemming from its strictly symmetrical structure, which reduces the experimental error arising from polarization deviation to verify the experimental stability and imbues it with the traits of convenience and practicability.

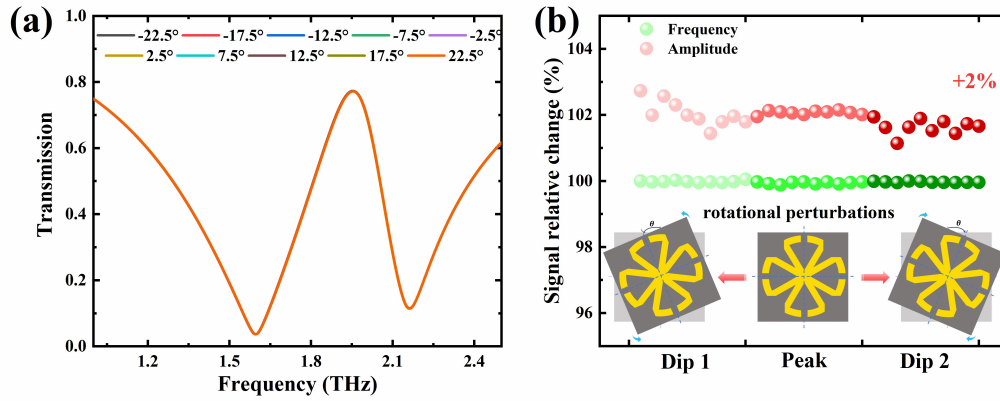


Fig. S2. (a) the transmission spectra and (b) corresponding signal relative change caused by rotational perturbations within  $45^\circ$ .

### Supplementary Fig. S3

The theoretical fitting and numerical simulation transmission spectra results of various  $d$  were shown in the Fig. S3 for comparison, which exhibited a well consistency and proved the effectiveness of the Lorentz oscillator model.

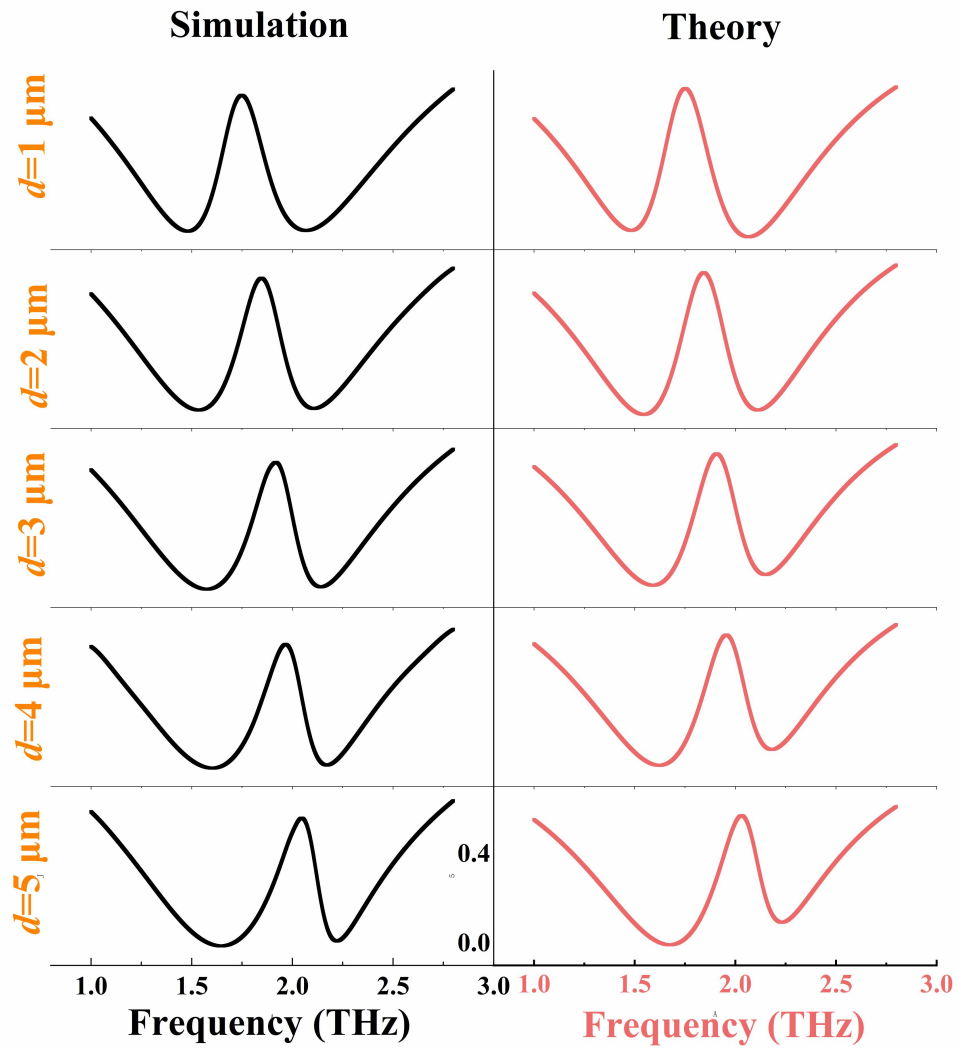


Fig. S3. The theoretical fitting and numerical simulation transmission spectra results of various  $d$ .